frontiers | Frontiers in Marine Science

TYPE Original Research
PUBLISHED 09 August 2022
DOI 10.3389/fmars.2022.960173



OPEN ACCESS

EDITED BY
John Everett Parkinson,
University of South Florida,
United States

REVIEWED BY
Virginia M Weis,
Oregon State University, United States
Dongxue Xu,
Qingdao Agricultural University, China

*CORRESPONDENCE
Liza M. Roger
rogerlm@vcu.edu;
liza.roger.research@gmail.com

SPECIALTY SECTION
This article was submitted to Marine Biology, a section of the journal Frontiers in Marine Science

RECEIVED 02 June 2022
ACCEPTED 13 July 2022
PUBLISHED 09 August 2022

CITATION
Roger LM, Russo JA, Jinkerson RE, Giraldo JP and Lewinski NA (2022) Engineered nanoceria alleviate thermally induced oxidative stress in free-living *Breviolum minutum* (Symbiodiniaceae, formerly Clade B). *Front. Mar. Sci.* 9:960173. doi: 10.3389/fmars.2022.960173



# Engineered nanoceria alleviates thermally induced oxidative stress in free-living *Breviolum minutum* (Symbiodiniaceae, formerly Clade B)

Liza M. Roger[1,2*], Joseph A. Russo[3,4], Robert E. Jinkerson[3,5], Juan Pablo Giraldo[5] and Nastassja A. Lewinski[1]

[1]Chemical and Life Science Engineering, Virginia Commonwealth University, Richmond, VA, United States, [2]Shool of Molecular Sciences, Arizona State University, Tempe, AZ, United States, [3]Chemical and Environmental Engineering, University of California Riverside, Riverside, CA, United States, [4]Microbiology, University of California Riverside, Riverside, CA, United States, [5]Botany and Plant Sciences, University of California Riverside, Riverside, CA, United States

The breakdown of symbiotic mutualism between cnidarian hosts and dinoflagellate algae partners (i.e., bleaching) has been linked to an immune-like response pathway brought on by a nitro-oxidative burst, a symptom of thermal stress. Stress induced by reactive oxygen species (ROS)/reactive nitrogen species is a problem common to aerobic systems. In this study, we tested the antioxidant effects of engineered poly(acrylic acid)-coated cerium dioxide nanoparticles ($CeO_2$, nanoceria) on free-living Symbiodiniaceae (*Breviolum minutum*), a dinoflagellate alga that forms symbiotic relationships with reef-building corals and anemones. Results show that poly(acrylic acid)-coated $CeO_2$ with hydrodynamic diameters of ~4 nm are internalized by *B. minutum* in under 30 min and subsequently localized in the cytosol. Nanoceria exposure does not inhibit cell growth over time, with the treated cultures showing a similar growth trend over the 25-day exposure. Aerobic activity and thermal stress when held at 34°C for 1 h (+6°C above control) led to increased intracellular ROS concentration with time. A clear ROS scavenging effect of the nanoceria was observed, with a 5-fold decrease in intracellular ROS levels during thermal stress. The nitric oxide (NO) concentration decreased by ~17% with thermal stress, suggesting the rapid involvement of NO scavenging enzymes or proteins within 1 h of stress onset. The presence of nanoceria did not appear to influence NO concentration. Furthermore, aposymbiotic anemones (*Exaiptasia diaphana*, ex *Aiptasia pallida*) were successfully infected with nanoceria-loaded *B. minutum*, demonstrating that inoculation could serve as a delivery method. The ability of nanoceria to be taken up by Symbiodiniaceae and reduce ROS production could be leveraged as a potential mitigation strategy to reduce coral bleaching.

KEYWORDS

**symbiotic dinoflagellate, antioxidant nanoparticles, cerium dioxide, reactive oxygen species (ROS), nitric oxide (NO), bleaching, Symbiodiniaceae, Cnidaria**

## Introduction

The symbiotic relationship between dinoflagellates of the family Symbiodiniaceae and reef-building corals (Scleractinia) is the keystone of tropical-subtropical reefs (Dubinsky, 1990; Weis, 2008). Regulatory crosstalk and partner recognition are essential to a successful balanced symbiosis and the associated nutritional exchanges (Weis, 2008). This is also the case in other cnidarians used as model species for the study of symbiosis such as Aiptasia (*Exaiptasia* spp.), *Anemonia viridis*, *Cassiopeia xamachana*, or Hydra. The specialized compartment that houses the endosymbiont inside the host cell, i.e., the symbiosome, acts as a complex signaling and trafficking interface with cell surface receptors and channels, e.g., G-protein-coupled receptors (GPCRs), lectins, scavenger receptors, toll-like receptors, nucleotide oligomerization domain (NOD)-like receptors, and Rhesus channels (Peng et al., 2010; Mansfield and Gilmore, 2019; Rosset et al., 2021; Thies et al., 2022).

Dysbiosis, or the breakdown of symbiotic mutualism, can be caused by abiotic and biotic factors, such as thermal stress, irradiance, alkalinity, salinity, viruses, and bacteria (van Oppen and Lough, 2018). The severity of dysbiosis and potential for recovery hinge on environmental history through frequency, intensity, amplitude, and nature of the stress applied to the holobiont (Krueger et al., 2015). In scleractinian corals, intense and prolonged exposure to elevated seawater temperatures, often combined with high UV radiations, can cause colony-scale dysbiosis, commonly referred to as "coral bleaching". If environmental stress is prolonged, it can result in coral death. Coral bleaching has been repeatedly observed on a global scale over the past couple of decades (Hoegh-Guldberg, 1999; McClanahan et al., 2007; Turner et al., 2020). Although the mechanisms of coral bleaching are not fully known, it is now understood that high concentrations of free radicals [reactive oxygen species (ROS) and reactive nitrogen species (RNS), together as nitro-oxidative stress], failing antioxidant machinery (e.g., catalase, ascorbate peroxidase, superoxide dismutase), and innate immune responses are key players in the breakdown of symbiosis through damage to cellular membranes, lipids, proteins, and DNA (Weis, 2008; Lesser, 2011).

A number of approaches have been tested to prevent bleaching from occurring with varying success, such as shading (Coelho et al., 2017), enhanced water circulation (Finelli et al., 2006), assisted evolution (van Oppen et al., 2015), preconditioning to promote thermal adaptation (Oliver and Palumbi, 2011), probiotic treatments (Peixoto et al., 2017; Rosado et al., 2019), and inoculation with more thermally resistant strains of dinoflagellates (Howells et al., 2012). Recent studies have also investigated the use of poly(ethylene glycol) (PEG)-encapsulated TEMPOL (a superoxide dismutase-mimicking drug) nanoparticles in *Acropora tenuis* coral larvae (Motone et al., 2018), as well as the microbiome bacteria-isolated antibiotic zeaxanthin in Symbiodiniaceae isolated from *Galaxea fascicularis* (Motone et al., 2020) to protect against the stress generated by abiotic factors with mixed success. While a 7-day exposure to PEG-TEMPOL nanoparticles increased larval survival at 33°C compared to TEMPOL and control, questions remain regarding larva settlement, metamorphosis, nanoparticle delivery, nanoparticle concentration, and survival assessment. Furthermore, although zeaxanthin treatment significantly decreased intracellular ROS concentration under thermal stress (6.5°C above normal temperature) and high irradiance (+150 µmol $m^{-2}$ $s^{-1}$ PAR above normal), survival rate and cytotoxicity data were not presented nor an *in hospite* comparison. These studies suggest that antioxidant-based bleaching mitigation strategies can be used to reduce ROS levels that may have a positive impact on coral-Symbiodiniaceae symbiosis subjected to thermal stress. However, these studies also suggest that the drug delivery mechanism is key and, as nanoparticles present high surface area-to-volume ratios, dose–response should be carefully tested for toxicity and potential growth impairments.

The work presented here tests the use of poly(acrylic acid)-coated cerium dioxide nanoparticles (hereafter referred to as "nanoceria" ) to mitigate nitro-oxidative stress in coral and anemone-associated, free-living, symbiotic dinoflagellate species *Breviolum minutum*, previously known as *Symbiodinium minutum* Clade B (LaJeunesse et al., 2018). Nanoceria are known for their free radical-scavenging properties and their chloroplast targeting in plants (Karakoti et al., 2008; Karakoti et al., 2010; Babu et al., 2010; Lee et al., 2013; Rico et al., 2013; Nelson et al., 2016; Wu et al., 2017; Gunawan et al., 2019; Mohammadi et al., 2021). Cultures of free-living *B. minutum* were dosed with nanoceria to assess internalization, growth response, and free radical-scavenging activity during thermal stress. The delivery of nanoceria to bleached anemone (*Exaiptasia diaphana*, ex *Aiptasia pallida*) by inoculation with nanoceria-loaded *B. minutum* was also explored.

## Materials and methods

### Nanoceria synthesis and characterization

Nanoceria synthesis followed the protocol developed by the Giraldo laboratory (Newkirk et al., 2018). Briefly, 108 mg of cerium (III) nitrate hexahydrate [$Ce(NO_3)_3 \bullet 6H_2O$, Sigma Aldrich, CAS Number 10294-41-4, MW 434.22 g/mol, 99% trace metal basis, SKU 238538-100G] was dissolved in 250 µl of molecular biology-grade water and combined with 45 mg of poly(acrylic)acid dissolved in 500 µl of molecular biology-grade water. After vortexing, the solution was added dropwise to 1.5 ml of 7.2 M ammonium hydroxide solution ($NH_4OH$, Fisher

Chemicals, Certified ACS Plus, FL-13-0907, MW 35.05 g/mol) under constant magnetic stirring (500 rpm, VWR® Standard hot plate stirrer) for 24 h at room temperature (22°C). The solution was centrifuged at 3,900 rpm [2,721 relative centrifugal force (RCF)] for 1 h to remove potential large agglomerates. The supernatant was then placed in 10 kDa Amicon® Ultra centrifuge filter with molecular biology-grade water and centrifuged at 3,900 rpm (2,721 RCF) for 15 min. The filtration/centrifugation process was repeated six times. This synthesis process generates a clear yellow colloidal solution of 1.3 M nanoceria.

The nanoparticle size was measured using dynamic light scattering (DLS; Malvern Zetasizer Nano) and transmission electron microscopy (TEM; Zeiss Libra 120, SPI #3520C-FA carbon-coated 200 mesh copper grids 3 mm) at the Virginia Commonwealth University Nanomaterials Core Characterization facility. Zeta potential (ζ) was calculated using electrophoretic light scattering (Malvern Zetasizer Nano) and the Smoluchowski approximation. UV-vis spectra were collected using a Perkin Elmer Lambda 35 at the University of California Riverside. For these analyses, the nanoparticle solution was diluted in different media (1:10): deionized water (pH 5.7), Marine Broth (pH 7.6, used for symbiotic dinoflagellate algae culture, see next section for details), and artificial seawater (pH 8). Analysis temperature was 27°C (*B. minutum* culture temperature).

## Symbiotic algae culture

Clonal and axenic cultures of the free-living symbiotic dinoflagellate, *B. minutum* (Clade B) strain SSB01, were cultured in the Jinkerson laboratory (University of California, Riverside) in a Percival I-36 VL incubator at 27°C with continuous light (24 h/day, 7 days/week, PAR: 5–10 µmol $m^{-2}$ $s^{-1}$) in culture medium made of 37.4 g Difco™ Marine Broth 2216 dissolved in 1 L of sterile Milli-Q water with final salinity of 30.3 ppt. During some experiments, *B. minutum* was suspended in calcium-, magnesium-free artificial seawater following the protocol reported by Domart-Coulon et al. (2001), with final salinity of 26.6 ppt.

## Internalization visualization

For visualization purposes, a fluorescent dye, 1,1'-dioctadecyl-3,3,3',3'-tetramethylindocarbocyanine perchlorate (DiI; Sigma Aldrich, CAS Number 41085-99-8, MW 933.87 g/mol, SKU 42364-100MG, ≥98% TLC), was encapsulated in the nanoceria. The DiI labeling followed the protocol developed by the Giraldo laboratory (Newkirk et al., 2018). Briefly, a staining solution of 1.6 mM DiI dissolved in Dimethyl sulfoxide (DMSO) was added dropwise to the 1.3 M colloidal solution of nanoceria under stirring at 1,000 rpm (VWR® Standard hot plate stirrer) over 1 min at room temperature (22°C). The stained solution was transferred to a 10 kDa Amicon® Ultra centrifuge filter with molecular biology-grade water to make up a total volume of 15 ml and centrifuged at 3,900 rpm (2,721 RCF) for 5 min. The filtration/centrifugation process was repeated five times.

The *B. minutum* cells exposed to DiI-labeled nanoceria were imaged using a Zeiss Laser Scanning Microscope 880, inverted confocal microscope (UCR Microscopy and Imaging Core Facility). The settings used for imaging are as follows: argon 488-nm laser excitation with collected emission wavelengths of 670–690 nm for chloroplast fluorescence; argon 514 nm laser excitation with collected emission wavelengths of 520–550 nm for DiI fluorescence.

To determine whether *B. minutum* could be used as a delivery agent to the cnidarian host, clonal aposymbiotic specimens of *E. diaphana* strain H2 were reared in the Jinkerson laboratory and were inoculated with nanoceria-loaded *B. minutum* (control n = 6, treatment n = 6). The inoculation method follows that developed by Jinkerson et al. (2022). Anemones used for inoculation were 3–5 mm in length (from the pedal disk to oral disk). Inoculation was performed in six-well polypropylene plates (one individual per well, 5.5 ml of artificial seawater per well). The inoculation mixture consisted of nanoceria-loaded algae (nanoceria concentration: 0.5 µg/ml; *B. minutum*: $1 \times 10^4$ cells/ml) mixed with decapsulated brine shrimp eggs (~26 mg/ml of seawater). The mixture was added to each well (500 µl of inoculation mixture per well) except the control well that received a mixture made of *B. minutum* ($1 \times 10^4$ cells/ml) mixed with decapsulated brine shrimp eggs (~26 mg/ml of seawater). Anemones were washed with artificial seawater after 24 h and transferred to a new six-well plate. All specimens were imaged under a fluorescence microscope (Keyence BZ-X710 all-in-one microscope with Texas Red filter for chlorophyll fluorescence visualization) prior to inoculation to confirm aposymbiotic status. They were then imaged again after 7 days (fluorescence microscope, Keyence BZ-X710) to determine whether inoculation was successful and infection had occurred. Finally, after 3 weeks, each individual was soaked in OCT medium (TissueTek, Sakura) for 24 h before freezing (-80° C) and cryosectioning (15-µm sections, Thermo Fisher Shandon Cryotome) at the VCU Microscopy Core.

The *E. diaphana* was sampled using laser ablation (ESI NWR193) as the front end of an inductively coupled plasma triple-quadrupole mass spectrometer (Agilent Technologies 8900). The sampling zone was targeted to be the tentacles of control and inoculated specimens, utilizing a spot size of 35 µm, with a power of 8 J/$cm^2$, rep rate of 30 Hz, and a dwell time of 30 s. After ablation, the samples were analyzed in MS/MS mode for $^{140}Ce$. For calibration, the National Institute of Standards and Technology (NIST) standards 614 and 612 were used.

## Growth and cytotoxicity experiments

Cultures were exposed to three different colloidal solutions: 1) synthesized DiI-labeled nanoceria, 2) synthesized unlabeled nanoceria, and 3) manufactured uncoated cerium dioxide ($CeO_2$, US Research Nanomaterials Inc., CAS 1306-38-3, stock US3037) all dispersed in Marine Broth. The concentrations tested were 0, 0.05, 0.125, 0.25, 0.5, and 1 µg/ml of the different colloidal solutions (three replicate plates with two wells per treatment, n = 6). The manufactured $CeO_2$ was previously characterized in the Lewinski laboratory (Figures S1A, B). The growth experiment was conducted in 96-well plates in triplicate under normal culture conditions (see section 2.2). Absorbance was measured every 5–7 days over 25 days at 750 nm using a microplate reader (BioTek/Agilent Technology SYNERGY H1) to determine variations in cell density. Absorbance was calibrated to cell density separately by measuring absorbance at 750 nm for different cell densities (Figure S1C).

## Free radical-scavenging assay

Before performing cellular assays, the antioxidant capacity of the nanoceria was tested using an acellular 2′,7′-dichlorodihydrofluorescein diacetate (DCFH-DA) assay based on the protocol reported by Zhao and Riediker (2014) (Full protocol available in S2).

Cells of *B. minutum* ($1 \times 10^6$ cells/ml) were loaded with fluorescent dyes, DCFH-DA designed for intracellular ROS detection and diaminofluorescein-2 diacetate (DAF-2 DA) designed for intracellular nitric oxide (NO; an RNS) detection. The cells were incubated in the dark for 1 h at room temperature with 10 mM DCFH-DA in Marine Broth (Gomes et al., 2005) and 8 µM DAF-2 DA in Ca–Mg-free seawater (Kojima et al., 1999; Bouchard and Yamasaki, 2009). The two separate samples were then centrifuged at 2,000 rpm (716 RCF) for 1 min at room temperature. The cells loaded with DCFH-DA were resuspended in fresh sterile Marine Broth, and cells loaded with DAF-2 DA were resuspended in Ca–Mg-free seawater for plating in a 96-well plate at 900,000 cells/well. The oxygen and nitrogen donors used as controls were hydrogen peroxide ($H_2O_2$; 0.1 µM –1 mM) and sodium nitroprusside (SNP; 0.1 µM –1 mM), respectively (Full ROS-NO protocols available in S2).

## Statistical analysis

Results were analyzed in R (version 4.1.1) using a number of statistical and imaging CRAN packages: ggplot2 (https://cran.r-project.org/package=ggplot2), ggpubr (https://cran.r-project.org/package=ggpubr), tidyverse https://cran.r-project.org/package=tidyversebroom (https://cran.r-project.org/package=broom), AICcmodavg (https://cran.r-project.org/package=AICcmodavg) Single-factor and two-factor ANOVAs were run depending on the nature of the data. To identify the best model between different interaction models or blocking model, in the case of two-way ANOVAs, the "aictab()" function was used, residuals of the best model were plotted, and Tukey *post-hoc* was generated (95% family-wise confidence level).

# Results

## Cerium dioxide nanoparticle characterization

Cell-to-nanomaterial interactions are controlled by nanoparticle properties (size, shape, charge, and composition) (Hu et al., 2020). DLS showed that both nanoceria and fluorescently (DiI) labeled nanoceria have an average particle size ranging from 1 to 6 nm (Figure 1A). Nanoparticle hydrodynamic diameter was measured in three different media: deionized water, seawater, and Marine Broth. TEM imaging indicated a 3.7 ± 0.1 nm size for DiI-labeled nanoceria (Figure 1B), and electron diffraction confirmed the polycrystalline structure of cerium oxide (Figure 1C). Absorbance of nanoceria labeled with DiI was lower in deionized water compared to that in Marine Broth (Figure 1D). The zeta potential (ζ) was found to be highly negative (-49.5 ± 3.1 mV) in deionized water (pH 5.7) and decreased as the ionic strength of the media increased, with ζ = -21.1 ± 2.5 mV in Marine Broth (pH 7.6) and ζ = -11.2 ± 0.6 mV in seawater (pH 8) (Figure 1E).

## Nanoparticle internalization by free-living algae

This study aimed to test the ROS- and RNS-scavenging effect of nanoceria on Symbiodiniaceae during thermal stress, thus the first step was to understand nanoceria internalization in live *B. minutum* cultures. Internalization guarantees the interaction of nanoceria with cell organelles directly producing ROS and RNS as opposed to cell surface adhesion. Laser scanning confocal microscopy revealed that the fluorescently labeled nanoparticles are internalized by the algal cells within 30 min of exposure in Marine Broth (Figure 2). The nanoceria appeared concentrated in the cytosol (Figure 2), and no colocalization with chloroplasts was observed. The negative control, no nanoparticle treatment (Figures 2E, F), confirmed that the detected nanoparticle fluorescence emission between 520 and 550 nm does not include endogenous fluorophores or background fluorescence in *B. minutum*.

The symbiotic relationship between Symbiodiniaceae and cnidarian is at the core of the current coral reef crisis. The

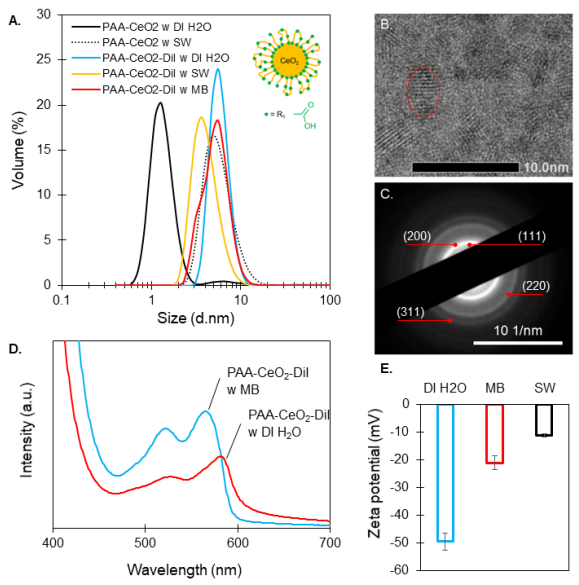


FIGURE 1
Characterization of $CeO_2$ nanoparticles. **(A)** Size distribution by volume (%) of poly(acrylic acid)-coated cerium dioxide (PAA-$CeO_2$; schematic representation of a coated nanoparticle) in deionized water (DI $H_2O$), seawater (SW), and PAA-$CeO_2$ labeled with DiI in DI $H_2O$, SW, and Marine Broth (MB) from dynamic light scattering. **(B)** Transmission electron microscopy (TEM) images showing lattice fringes of nanoceria (nanoparticles circled in red). **(C)** Ring diffraction pattern of nanoceria with Miller indices (TEM). **(D)** Absorbance of PAA-$CeO_2$ labeled with DiI in DI $H_2O$ and in MB. **(E)** Zeta potential ± standard error of PAA-$CeO_2$ labeled with DiI in DI $H_2O$, MB, and SW at 27°C.

development of a potential treatment for thermally induced dysbiosis needs to consider the treatment delivery method. Here, we tested inoculation and infection of aposymbiotic *E. diaphana* with nanoceria-loaded *B. minutum* as a treatment delivery method. Fluorescence imaging of the inoculated *E. diaphana* showed successful infection of the tissue by *B. minutum* (using chlorophyll fluorescence); all control specimens and all treatment specimens were successfully infected (Figure 3). However, colocalization of the nanoparticles inside the algae inside the anemone tissue after 3 weeks was not possible using fluorescence microscopy (DiI fluorescence absent). During these 3 weeks, the algae grew and divvied several times, which may have reduced the fluorescence signal of the nanoceria to below levels we could detect. Notwithstanding, we confirmed internalization of nanoceria by the anemones inoculated with nanoceria-loaded *B. minutum* using laser ablation inductively couple plasma mass spectrometry (LA ICP MS, measuring cerium $^{140}Ce$ in the tentacles of control and inoculated anemones compared to standards NIST614 and NIST612, S3).

## Growth experiment

Algae cell culture growth can be assessed by determining their cell density *via* absorbance measurements (optical density) (Moheimani et al., 2013). Measuring the absorbance at wavelengths of 550 or 750 nm is preferred to avoid chlorophyll and other pigment interferences (Moheimani et al., 2013). Considering that the DiI-labeled nanoceria have absorbance peaks between 300 and 400 nm ($CeO_2$) and 460 and 590 nm (DiI label) (Newkirk et al., 2018), absorbance at 750 nm was chosen for this study. Calibration of the relationship between absorbance and *B. minutum* cell density is presented in S1C. *B. minutum* SSB01 cells have an overall slow growth rate, ~0.09 over a 25-day period (Xiang et al., 2013). Calculated average growth rates [K' (Levasseur et al., 1993)] show that all cultures, except that exposed to nanoceria concentration of 1 µg/ml (all three types of nanoceria), grew similarly to control over the 25-day period of exposure (K' 0.13 ± 0.008 per day, Figure 4). Only the highest concentration for all three nanoceria tested (1 µg/ml) corresponded to significantly higher culture growth rates (av. K' 0.16 ± 0.003 per day) relative to control (av. K' 0.13 ± 0.008 per day).

## Free radical-scavenging assay

We confirmed the ROS-scavenging capacity of nanoceria (acellular scavenging) at concentrations ranging from 6.25 to 100 µg/ml (nanoceria concentration) in the presence of 1 mM hydrogen peroxide (S4). Intracellular ROS levels in *B. minutum* increased over the 60 min experiment in all treatments [cell-only (-)CTL, 100µM $H_2O_2$ treatment (+)CTL, and 1.8 µM nanoceria treatment ($CeO_2$)] at both temperatures tested (27°C: normal culture temperature and 34°C: thermal stress, S5). Intracellular ROS levels in the cell-only control treatment (-)CTL at the 60 min time point were significantly higher at 34°C compared those in the normal culture temperature (27°C) (Figure 5A, S7). A significant decrease in intracellular ROS was found between the cell-only control treatment and the 1.8 µM nanoceria treatment at both temperatures tested (Figure 5A, S7). The intracellular ROS level in the 100-µM $H_2O_2$ treatment showed a significant decrease between the control temperature (27°C) and the thermal stress treatment 34°C (Figure 5A, S7). In summary, intracellular ROS concentration increased with thermal stress. The addition of 100 µM $H_2O_2$ to the cultures also increased intracellular ROS levels at 27°C but not at 34°C. At both temperatures tested, nanoceria successfully scavenged the intracellular ROS in *B. minutum*.

We also evaluated the ability of the nanoceria to scavenge intracellular NO using SNP (1 µM) as an NO donor during normal growth conditions and thermal stress. The intracellular

10.3389/fmars.2022.960173

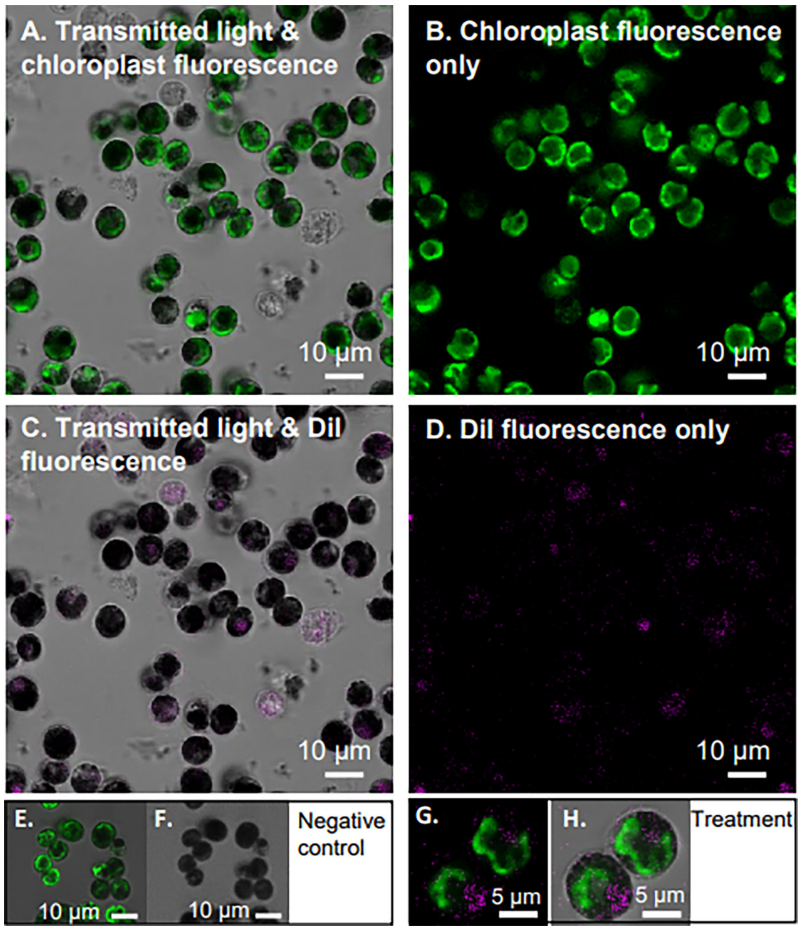


FIGURE 2
Internalization of nanoceria by *Breviolum minutum*. Confocal microscopy images of *B. minutum* exposed to DiI-labeled nanoceria (325 mM final concentration). Internalization occurred in under 30 min post-exposure. Panels **(A–D)** show the same view with different filters applied (see *Materials and Methods*) to highlight cell chloroplast in green and nanoceria in magenta. Transmitted light in turn is displayed **(A, C)** or not **(B, D)** for contrast. Images of negative control are also displayed **(E, F)**. Enlarged view of two *B. minutum* cells with internalized DiI-labeled nanoceria **(G, H)**. Scale bars: **(A–F)** 10 µm; **(G, H)** 5 µm.

NO levels in *B. minutum* at the 60 min time point in the cell-only treatment was higher (median) in the cultures exposed to thermal stress compared to the control temperature treatment (Figure 5B, S7), but not significantly. When exposed to 1 µM SNP and thermal stress, the intracellular NO levels significantly decreased compared to control temperature (Figure 5B, S7). When exposed to 1.8 µM of nanoceria, intracellular NO levels were not significantly different from the cell-only control at 27°C but were significantly lower at 34°C (Figure 5B, S7). Overall, thermal stress did not generate a significant increase in intracellular NO. The addition of the NO donor (SNP) did not significantly increase the intracellular NO levels at 27°C, but these levels significantly decreased at 34°C; levels were also significantly different (higher) in the positive control treatment between the cultures exposed to normal culture temperature compared to thermal stress. The nanoceria treatment significantly decreased intracellular NO levels during thermal stress but not at normal culture temperature.

To assess the relationship between intracellular ROS and NO levels of *B. minutum*, covariance was tested (Figure 6). The cell-only control revealed a positive relationship between intracellular levels of ROS and NO at 27°C, but no relationship was found at 34°C (Figures 6A, B). The positive control treatments that consisted of the addition of 100 µM $H_2O_2$ and 1 µM SNP showed a negative relationship between intracellular ROS and NO levels at 34°C (no significant relationship was found at 27°C; Figures 6C, D). Finally, when exposed to nanoceria, intracellular levels of ROS and NO were not significantly correlated in either of the thermal culture conditions (Figures 6E, F). It should be noted that all levels increased over time, from the 5 min time point to the 60 minute time point.

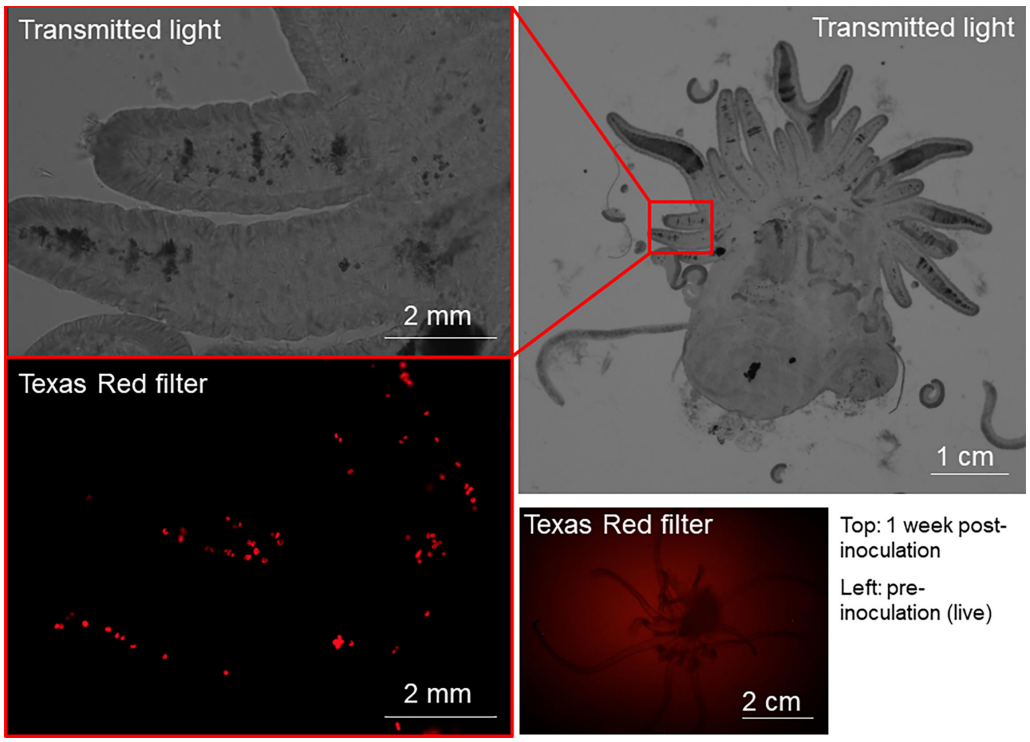


FIGURE 3
Microscopy images of *E. diaphana* pre- and post-inoculation with nanoceria-loaded *B. minutum*. The bottom right panel shows a long-exposure fluorescent image of a specimen of *E. diaphana* prior to inoculation using the Texas Red filter to visualize algae chlorophyll fluorescence. No algae are visible in the anemone, confirming its aposymbiotic state. The other three panels show the same specimen 1 week after inoculation with nanoceria-loaded *B. minutum* in transmitted light (top two panels) and Texas Red filter (bottom left panel). Algae chlorophyll fluorescence is visible in the bottom left panel, thereby confirming successful infection by *B. minutum*.

# Discussion

## Nanoceria internalization and culture growth

Nanoceria cell surface agglomeration was not visible, suggesting that nanoceria do not generate a shading effect (Navarro et al., 2008). Shading by nanoparticles would affect the photosynthetic efficiency of the algae. Nanoceria were rapidly internalized by *B. minutum* (Figure 2), although the delivery to the chloroplast as described in plants in Wu et al. (2017) was not observed. Nanoceria internalization into the cytosol is likely facilitated by the small size of the nanoparticles, which can pass through the algae cell wall pores [5–20 nm (Wang et al., 2019)], and the negative ζ potential (-21.1 ± 2.5 mV in Marine Broth) that allows penetration through the cell membrane. It has been reported that nanoparticles can aggregate in the cell membrane of freshwater algae, causing membrane damage and cell apoptosis (Bhuvaneshwari et al., 2015; Wang et al., 2019). Herein, nanoceria do not appear to be trapped in the cell wall of *B. minutum* (Figure 2) but rather concentrated in the cytosol, occupying the chloroplast-free space. Previous studies of nanoparticle uptake in plant cells reported that nanomaterials require a higher zeta potential magnitude than 30 mV to enter chloroplasts, and that 20 mV is the minimum magnitude required for uptake in the cytosol (Wong et al., 2016; Lew et al., 2018), which explains why the nanoceria synthesized in this study did not enter the chloroplasts. Systematic studies on the role of nanoparticle size and charge on algae uptake are needed to determine if a similar threshold of zeta potential limits their translocation across cell and chloroplast lipid membranes.

The three types of nanoceria (commercially purchased uncoated cerium dioxide, PAA-coated cerium dioxide, and PAA-coated DiI-labeled cerium dioxide) tested on cultures of *B. minutum* (Figure 4) were chosen to demonstrate that nanoparticle coating is an important part of their engineering and how they interact with biological systems. All three types of $CeO_2$ nanoparticles allowed cell population growth over time (Figure 4), and growth rates were similar to that of control. The only statistically significant density increase compared to control, after 25 days, was found in cultures exposed to 1 μg/ml of nanoceria (all three types).

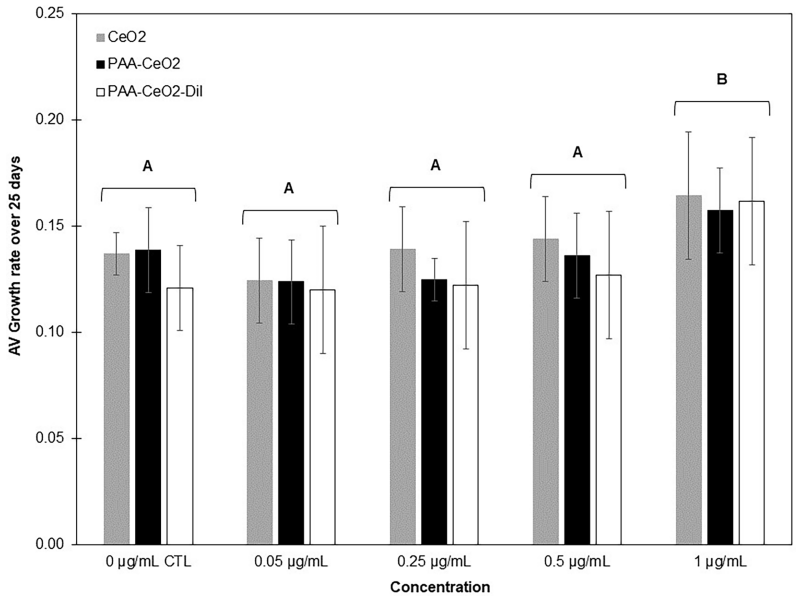


FIGURE 4
Average *B. minutum* growth rate ( ± SD, calculated from the absorbance measured at 750 nm and calibration curve, S1C) exposed to concentrations of commercially purchased uncoated nanoceria ($CeO_2$), PAA-coated nanoceria (PAA-$CeO_2$), and PAA-coated nanoceria with DiI label (PAA-$CeO_2$-DiI) between 0.05 and 1 µg/ml (+ control) for 25 days (three replicate plates with two wells per treatment, n = 6 for each treatment). Groups with different letters are significantly different (single-factor ANOVA). Growth rate was not significantly different between different types of nanoceria at the same concentrations. Average K′ values per day in the different treatments were as follows: control K′ 0.13 ± 0.008, 0.05 µg/ml K′ 0.14 ± 0.01, 0.25 µg/ml K′ 0.12 ± 0.01, 0.5 µg/ml K′ 0.13 ± 0.01, 1 µg/ml K′ 0.16 ± 0.003.

Aposymbiotic specimens of *E. diaphana* showed successful infection by *B. minutum* and nanoceria-loaded *B. minutum*, but colocalization of the nanoparticles inside the algae within the anemones could not be observed using fluorescence microscopy. The cause for this complication can be explained by the extended period of time the dye-labeled nanoceria were exposed to light inside the anemones (3 weeks) before preservation for later analysis, which can cause photobleaching of the DiI fluorophore. Regardless of this setback, colocalization was successfully confirmed using LA ICP MS (S3), further supporting inoculation and infection as a method to deliver nanoparticle-based treatments to *E. diaphana*.

## Reactive oxygen species and nitric oxide in free-living *Breviolum minutum*

The concentrations of $H_2O_2$ chosen for this experiment are based on the work by Diaz et al. (2016) where they measured the $H_2O_2$ concentration in bleached *Pocillopora damicornis* corals as a measure of ROS at ~0.5 µg/ml. The nanoceria concentrations tested were chosen assuming a potential one-to-one relationship between ROS production and nanoceria quenching. The nanoceria concentrations were then mirrored in the NO experiments for consistency.

The intracellular ROS concentration in free-living *B. minutum* indicated by DCF fluorescence increased over the 1 h period of measurement (~2.88 times more at 60 min compared to 5 min) at normal culture temperature (27°C) due to the standard aerobic metabolic activities of the cells (S5), i.e., respiration and photosynthesis, which continuously produce ROS as by-products. A similar trend is observed at 34°C but associated with a lower overall ROS concentration. At the 1 h time point, intracellular ROS levels are significantly higher in cultures under thermal stress compared to those grown under normal culture temperature (Figure 5A). While much higher concentrations were expected during thermal stress, the trend observed could be the result of antioxidant enzyme upregulation (superoxide dismutase, ascorbate peroxidase, and catalase peroxidase) as demonstrated by Krueger et al. (2015) or lipid peroxidation (malondialdehyde), but more work is needed to confirm this. The results presented here suggest that lipid peroxidation and/or antioxidant enzymes are upregulated early when *B. minutum* is exposed to acute thermal stress, within 1 h at 34°C. This also appears to be the case in the cultures treated with 100 µm $H_2O_2$ exposed to 34°C for 1 h.

The intracellular NO concentration in free-living *B. minutum* indicated by DAF-2 fluorescence is stable over the 1 h period of measurement (~4 × $10^6$ a.u., cell-only control, S5) but highly variable at each SNP concentration over the same

10.3389/fmars.2022.960173

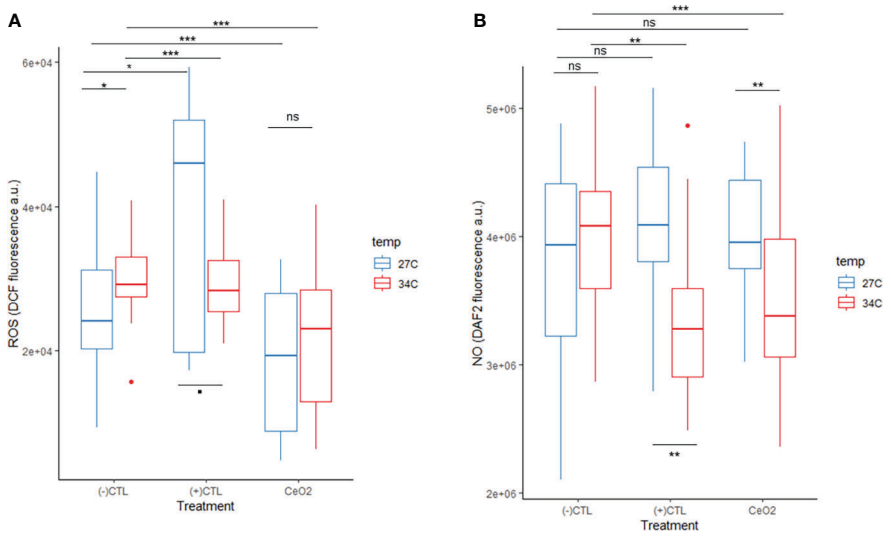


FIGURE 5
*B. minutum* reactive oxygen species level (ROS level indicated by DCF fluorescence) at 27°C and 34°C in the cell-only control [(-)CTL treatment], when exposed to 100 µM $H_2O_2$ [(+)CTL treatment], and when exposed to 1.8 µM nanoceria ($CeO_2$ treatment) at the 60-min time point **(A)**. *B. minutum* nitric oxide level (NO level indicated by DAF2 fluorescence) at 27°C and 34°C in the cell-only control [(-)CTL treatment], when exposed to 1 µM SNP [(+)CTL treatment], and when exposed to 1.8 µM nanoceria ($CeO_2$ treatment) at the 60-min time point **(B)**. A total of seven assays were run at 27°C and four at 34°C for both ROS and NO detection. Each assay at 27°C had three internal replicates for the $CeO_2$ and the (+)CTL treatments and six for the (-)CTL treatment [$CeO_2$ n = 21, (+)CTL n = 21, (-)CTL n = 42]. A total of four assays were run at 34°C. Each assay at 34°C had three internal replicates for the $CeO_2$ and the (+)CTL treatments and six for the (-)CTL treatment [$CeO_2$ n = 12, (+)CTL n = 12, (-)CTL n = 24]. Boxes summarize data spread with line (median), whiskers (min–max), and dots (outliers). Two-way ANOVA p-value significant levels presented on graphs as: "ns" for p-value >0.05, "." for p-value between 0.05 and 0.01, "*" for p-value between 0.01 and 0.001, "**" for p-value between 0.001 and 0, and "***" for p-value = 0. See S4 and S5 for supplementary graphs and statistical analysis results.

period (overall stable average) at normal culture temperature (27°C). The absence of a significant increase in intracellular NO levels between control temperature and thermal stress (34°C) in the cell-only control and 1 µM SNP treatments, Figure 5B, is likely caused by the reaction of NO with superoxide to form peroxynitrite ($\bullet NO + O_2^{\bullet -} \rightarrow ONOO^-$). This reaction is favored over the dismutation of superoxide (SOD, superoxide dismutase enzyme catalyst) that would leave NO free to activate DAF-2T fluorescence due to a reaction rate constant one order of magnitude higher than the formation of $H_2O_2$ by SOD catalysis (Radi, 2018). The fluorescence of DAF-2T does not increase because NO is likely hijacked to form peroxynitrite with superoxide. Peroxynitrite is a potent nitro-oxidative agent with high diffusibility that can affect cells within a ~5–20 µm radius (Marla et al., 1997; Szabó et al., 2007). Peroxynitrite can cause lipid peroxidation, protein modifications, and DNA damage in plant cells by oxidation or nitration (Vandelle and Delledonne, 2011). This is also observed in the NO-positive control treatments where NO donor SNP was added with a significant decrease of intracellular NO levels as indicated by DAF2 fluorescence (Figure 5B). Recently discovered hemoglobin-like proteins (Hb) in symbiotic dinoflagellates could also be the cause for the NO decrease with thermal stress since these Hbs are known NO scavengers (Rosic et al., 2013). Rosic et al. (2013) only found significant changes in Hb levels related to thermal stress when symbiotic algae were associated with their coral partners; nevertheless, the stress applied to both free-living cultures and holobionts was not as acute as that applied here, suggesting that the stress response was not detected by Rosic et al. Another potential cause for lower levels of NO during thermal stress with added NO (SNP) could be the upregulation of nitric oxide synthase or the formation of thionitrites (S-nitrosothiols) (Parankusam et al., 2017).

Using SNP [molecular formula: $Na_2Fe(CN)_5NO.2H_2O$] as an NO donor should be carefully considered due to its dissociation process. During decomposition, SNP generates 5 moles of cyanide for 1 mole of NO, which could cause cell death. Certain concentrations of SNP might also lead to excess peroxynitrite ($ONOO^-$) and peroxynitrous acid (ONOOH) formation with the associated negative effects on cells in the absence (or low level) of the anti-nitro-oxidant enzymes and proteins typically upregulated at high temperatures. Testing for these proteins and enzymes was outside the scope of this study, but it is apparent that these endpoints should be included in future work to understand the mechanisms of ROS and NO production in symbiotic dinoflagellates.

10.3389/fmars.2022.960173

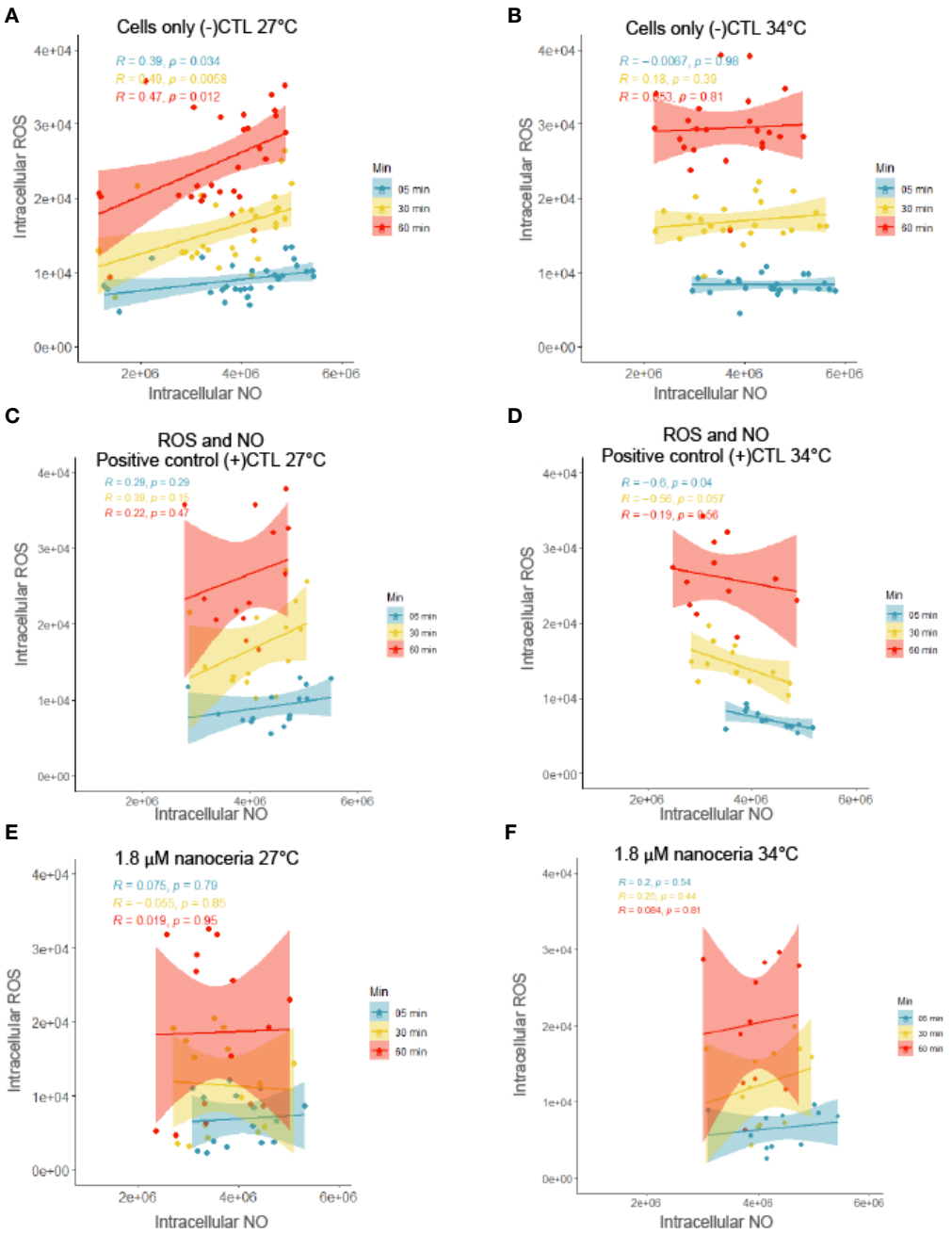


FIGURE 6
Relationship between intracellular ROS and NO levels in *B. minutum* in the cell-only control at 27°C **(A)** and 34°C **(B)**; in the presence of added ROS (1 µM $H_2O_2$) and NO (1 µM SNP) at 27°C **(C)** and 34°C **(D)**; in the presence of 1.8 µM nanoceria at 27°C **(E)** and 34°C **(F)**. Linear correlation between ROS and NO levels presented in each graphic with residuals (R) and p-value (*p*). [Data used here were the same as in Figure 5 so at 27°C $CeO_2$ n = 21, (+)CTL n = 21, (-)CTL n = 42 and at 34°C $CeO_2$ n = 12, (+)CTL n = 12, (-)CTL n = 24.].

## Scavenging of reactive oxygen species and nitric oxide by nanoceria

Levels of ROS were lower in free-living *B. minutum* exposed to nanoceria than those in nanoparticle-free controls, demonstrating an antioxidant effect of the nanoceria at all concentrations tested (Figure 5A). The thermal stress added by exposure to 34°C for 1 h also showed clear differences compared to control and normal culture conditions (Figure 5A), suggesting that the ROS burst caused by thermal stress (+6°C) can be

counteracted by the scavenging activity of poly(acrylic acid)-coated cerium dioxide. The application of antioxidant nanoceria to free-living symbiotic dinoflagellates to treat oxidative stress has clear potential as demonstrated in this study. Symbiodiniaceae tolerance to environmental stress has been mostly studied in free-living conditions in contrast with *in hospite* in dissociated cnidarian tissue or intact organisms (Roger et al., 2021), with findings deviating from the holobiont response to thermal stress. The hypersensitivity of the holobiont appears to be due to the dynamic equilibrium between negative and positive feedback loops involving hosts and symbionts [e.g., nutrient cycling feedback loop (Rädecker et al., 2021)]. The present study and current experimental methods have their limitations; nevertheless, it is important to combine *in vitro* (free-living) testing with *in hospite* experimentation to understand the implications on symbiosis. The logical next step is to confirm these findings with *in hospite* testing.

The dynamics involved with NO production and scavenging are more complex than that of ROS. NO pathways in higher plants (Parankusam et al., 2017; Kohli et al., 2019) and freshwater algae (especially *Chlamydomonas reinhardtii*) (Astier et al., 2021) have been studied more extensively in comparison to symbiotic algae (free-living and *in hospite*). The oxidation of NO (to nitrite or nitrate) in thermally stressed, *in hospite* endosymbionts has been linked to bleaching as an immune-like response associated with host cell apoptosis signaling (Hawkins et al., 2014). The production of NO is concentrated in host cells of stressed anemone holobionts, as opposed to their endosymbionts (Perez and Weis, 2006), suggesting the host as the source of NO production (Perez and Weis, 2006; Mansfield and Gilmore, 2019). This could explain the lack of thermally induced significant NO increase found in our study overall. Nanoceria show NO-scavenging activity during thermal stress despite unexpected control treatment results (Figure 5B). *In hospite* testing of NO in the presence of nanoceria will help determine with more certainty their effect on NO levels under normal and stressful growth conditions, and nanoceria-loaded endosymbionts could help confirm the source of NO production during physiological stress.

## Nanoceria and bleaching future perspectives

Treating heat-induced nitro-oxidative stress using nanoceria has potential for further applications in marine algae. Inoculation of nanoceria-loaded Symbiodiniaceae (*B. minutum*) resulted in a successful infection of Aiptasia, and nanoceria colocalization was confirmed by LA ICP MS. Our findings suggest that nanoceria can address the ROS burst generated by acute thermal stress without increasing the NO levels. More studies are needed to better understand the fundamental mechanisms involved in NO generation, signaling pathways, and scavenging in symbiotic algae and cnidarians. Before large-scale application can be considered, the effects of nanoceria on cnidarians, endosymbionts, other marine taxa, and the marine environment as a whole need to be better understood and characterized (i.e., bioaccumulation, residence time, fate, cycling, and potential trophic transfer).

Cerium dioxide nanoparticles are already introduced to the environment by motor vehicle exhaust (fuel additives), electronic waste, recycling of sewage, and wastewater runoff (Dahle and Arai, 2015; Dedman et al., 2021). To date, studies suggest that environmental risks associated with nanoceria are low (Dedman et al., 2021) but limited data exist with regard to the marine environment. Our study is the first investigating the effects of nanoceria on marine dinoflagellates (Symbiodiniaceae). Marine microorganisms with high surface area-to-volume ratios could be at higher risk, especially in coastal regions (Lucas et al., 2011; Dedman et al., 2021). Considering that these organisms represent the heart of the marine food web, it is critical to better characterize these interactions. Marine cyanobacteria (*Prochlorococcus*) showed an initial short-term growth inhibition (72 h) at a high nanoceria concentration (100 µg/ml, ~20 ± 12.1 nm, heterogeneous morphology: cuboids, diamond- and triangular-shaped particles) attributed to aggregation (between nanoparticles and between nanoparticles and cells) rather than cell death (Dedman et al., 2021). Results by Dedman et al. (2021) confirm previous findings that suggest that surface interaction and sedimentation/agglomeration of nanoparticles could be the main dynamic in freshwater (Van Hoecke et al., 2011) and marine systems (Deng et al., 2017). However, delivering antioxidant nanoceria at low concentrations by reinfection would circumvent these issues. Upcoming tests will confirm whether the antioxidant effect of nanoceria is preserved with reinfection and prevents/mitigates cnidarian thermal stress-induced bleaching at the holobiont scale. Furthermore, assuming that the antioxidant effect is conserved by symbiotic algae when symbiosis is (re)established, this nanoceria treatment could be applied preventively, reliant on endosymbiont shuffling and switching (Boulotte et al., 2016).

# Conclusions

The development of therapeutic nanoparticles is an area of intense study in human medicine and agriculture for targeted drug delivery and for protection against infections and parasites. We believe that engineered nanoparticles can also be applied as therapeutics to heal marine ecosystems. The work presented here involves treating nitro-oxidative stress, a symptom of environmental stress and bleaching, using engineered antioxidant nanoparticles made of cerium oxide. With this aim, we tested the internalization and effect on growth and on intracellular ROS and NO levels of nanoceria in free-living symbiotic dinoflagellates *B. minutum*.

Nanoceria internalization was rapid and most likely facilitated by the small size of the nanoparticles. Cell density growth benefited from nanoceria addition as did ROS levels (ROS-scavenging). Nanoceria lowered intracellular NO concentration during thermal stress, but confounding results in the control treatments could indicate a rapid activation of NO-scavenging enzymes and proteins. Finally, anemone infection of nanoceria-loaded *B. minutum* was successful, which paves the way to testing the response to thermal stress of these new antioxidant anemone holobionts. Future work will consist of additional endpoints such as enzyme and protein concentration measurements, investigating the delivery of nanoceria to coral cells, and applying thermal stress to infected anemones and corals to test this nanoceria treatment approach in coral bleaching.

## Data availability statement

The datasets presented in this study can be found in online repositories. The names of the repository/repositories and accession number(s) can be found in the article/Supplementary Material.

## Author contributions

Conceptualization: LR, NL, JPG, RJ; Data curation: LR; Formal analysis: LR; Funding acquisition: LR, NL, JPG, RJ; Investigation: LR; Methodology: LR, NL, JPG, RJ, JR; Project administration: LR; Resources: NL, JPG, RJ; Supervision: NL, JPG, RJ; Validation: LR; Visualization: LR, JR; Writing – original draft: LR, NL, JPG, RJ, JR; Writing – review & editing: LR.

## Funding

This material is based upon work supported by the National Science Foundation under NSF Award Number 1939699 (NL, LR), the Coral Bleaching RCN Early Career Training Program NSF grant number 1838667 (LR), and University of California, Riverside College of Natural and Agriculture Sciences (J-PG) and Bourns College of Engineering (RJ, JR).

## Acknowledgments

The authors would like to thank all contributors to the Synthetic Coral HDR project. We thank John Cuddehe for characterizing the manufactured cerium oxide nanoparticles. We also are grateful to Dr. Joseph Turner for his assistance collecting the LA-ICP-MS data.

## Conflict of interest

The authors declare that the research was conducted in the absence of any commercial or financial relationships that could be construed as a potential conflict of interest.

## Publisher's note



## Supplementary material

The Supplementary Material for this article can be found online at: https://www.frontiersin.org/articles/10.3389/fmars.2022.960173/full#supplementary-material

## References

Astier, J., Rossi, J., Chatelain, P., Klinguer, A., Besson-Bard, A., Rosnoblet, C., et al. (2021). Nitric oxide production and signalling in algae. *J. Exp. Bot.* 72, 781–792. doi: 10.1093/jxb/eraa421

Babu, S., Cho, J.-H., Dowding, J. M., Heckert, E., Komanski, C., Das, S., et al. (2010). Multicolored redox active upconverter cerium oxide nanoparticle for bio-imaging and therapeutics. *Chem. Commun.* 46, 6915–6917. doi: 10.1039/c0cc01832e

Bhuvaneshwari, M., Iswarya, V., Archanaa, S., Madhu, G. M., Kumar, G. K. S., Nagarajan, R., et al. (2015). Cytotoxicity of ZnO NPs towards fresh water algae scenedesmus obliquus at low exposure concentrations in UV-c, visible and dark conditions. *Aquat. Toxicol.* 162, 29–38. doi: 10.1016/j.aquatox.2015.03.004

Bouchard, J. N., and Yamasaki, H. (2009). Implication of nitric oxide in the heat-stress-induced cell death of the symbiotic alga symbiodinium microadriaticum. *Mar. Biol.* 156, 2209–2220. doi: 10.1007/s00227-009-1249-3

Boulotte, N. M., Dalton, S. J., Carroll, A. G., Harrison, P. L., Putnam, H. M., Peplow, L. M., et al. (2016). Exploring the symbiodinium rare biosphere provides evidence for symbiont switching in reef-building corals. *ISME J.* 10, 2693–2701. doi: 10.1038/ismej.2016.54

Coelho, V. R., Fenner, D., Caruso, C., Bayles, B. R., Huang, Y., and Birkeland, C. (2017). Shading as a mitigation tool for coral bleaching in three common indo-pacific species. *J. Exp. Mar. Biol. Ecol.* 497, 152–163. doi: 10.1016/j.jembe.2017.09.016

Dahle, J. T., and Arai, Y. (2015). Environmental geochemistry of cerium: Applications and toxicology of cerium oxide nanoparticles. *Int. J. Environ. Res. Public Health* 12, 1253–1278. doi: 10.3390/ijerph120201253

Dedman, C. J., Rizk, M. M. I., Christie-Oleza, J. A., and Davies, G.-L. (2021). Investigating the impact of cerium oxide nanoparticles upon the ecologically significant marine cyanobacterium prochlorococcus. *Front. Mar. Sci.* 8. doi: 10.3389/fmars.2021.668097

Deng, Y., Ren, J., Guo, Q., Cao, J., Wang, H., and Liu, C. (2017). Rare earth element geochemistry characteristics of seawater and porewater from deep sea in western pacific. *Sci. Rep.* 7, 16539. doi: 10.1038/s41598-017-16379-1

Diaz, J. M., Hansel, C. M., Apprill, A., Brighi, C., Zhang, T., Weber, L., et al. (2016). Species-specific control of external superoxide levels by the coral holobiont during a natural bleaching event. *Nat. Commun.* 7, 1–10. doi: 10.1038/ncomms13801

Domart-Coulon, I. J., Elbert, D. C., Scully, E. P., Calimlim, P. S., and Ostrander, G. K. (2001). Aragonite crystallization in primary cell cultures of multicellular isolates from a hard coral, pocillopora damicornis. *Proc. Natl. Acad. Sci. U.S.A.* 98, 11885. doi: 10.1073/pnas.211439698

Dubinsky, Z. (1990). Coral Reefs. (Amsterdam; New York: Elsevier)

Finelli, C. M., Helmuth, B. S. T., Pentcheff, N. D., and Wethey, D. S. (2006). Water flow influences oxygen transport and photosynthetic efficiency in corals. *Coral Reefs* 25, 47–57. doi: 10.1007/s00338-005-0055-8

Gomes, A., Fernandes, E., and Lima, J. L. (2005). Fluorescence probes used for detection of reactive oxygen species. *J. Biochem. Biophys. Methods* 65, 45–80. doi: 10.1016/j.jbbm.2005.10.003

Gunawan, C., Lord, M. S., Lovell, E., Wong, R. J., Jung, M. S., Oscar, D., et al. (2019). Oxygen-vacancy engineering of cerium-oxide nanoparticles for antioxidant activity. *ACS Omega* 4, 9473–9479. doi: 10.1021/acsomega.9b00521

Hawkins, T. D., Krueger, T., Becker, S., Fisher, P. L., and Davy, S. K. (2014). Differential nitric oxide synthesis and host apoptotic events correlate with bleaching susceptibility in reef corals. *Coral Reefs* 33, 141–153. doi: 10.1007/s00338-013-1103-4

Hoegh-Guldberg, O. (1999). Climate change, coral bleaching and the future of the world's coral reefs. *Mar. Freshw. Res.* 50, 839–866. doi: 10.1071/MF99078

Howells, E., Beltran, V., Larsen, N., Bay, L., Willis, B., and Van Oppen, M. (2012). Coral thermal tolerance shaped by local adaptation of photosymbionts. *Nat. Climate Change* 2, 116–120. doi: 10.1038/nclimate1330

Hu, P., An, J., Faulkner, M. M., Wu, H., Li, Z., Tian, X., et al. (2020). Nanoparticle charge and size control foliar delivery efficiency to plant cells and organelles. *ACS Nano* 14, 7970–7986. doi: 10.1021/acsnano.9b09178

Jinkerson, R. E., Russo, J. A., Newkirk, C. R., Kirk, A. L., Chi, R. J., Martindale, M. Q., et al. (2022). Cnidarian-symbiodiniaceae symbiosis establishment is independent of photosynthesis. *Curr. Biol* 32 (11), 2402–2415.e4. doi: 10.1016/j.cub.2022.04.021

Karakoti, A., Monteiro-Riviere, N., Aggarwal, R., Davis, J., Narayan, R., Self, W., et al. (2008). Nanoceria as antioxidant: synthesis and biomedical applications. *Jom* 60, 33–37. doi: 10.1007/s11837-008-0029-8

Karakoti, A., Singh, S., Dowding, J. M., Seal, S., and Self, W. T. (2010). Redox-active radical scavenging nanomaterials. *Chem. Soc. Rev.* 39, 4422–4432. doi: 10.1039/B919677N

Kohli, S. K., Khanna, K., Bhardwaj, R., Abd_Allah, E. F., Ahmad, P., and Corpas, F. J. (2019). Assessment of subcellular ROS and NO metabolism in higher plants: Multifunctional signaling molecules. *Antioxidants* 8, 641–668. doi: 10.3390/antiox8120641

Kojima, H., Urano, Y., Kikuchi, K., Higuchi, T., Hirata, Y., and Nagano, T. (1999). Fluorescent indicators for imaging nitric oxide production. *Angew. Chem. Int. Ed.* 38, 3209–3212. doi: 10.1002/(SICI)1521-3773(19991102)38:21%3C3209::AID-ANIE3209%3E3.0.CO;2-6

Krueger, T., Hawkins, T. D., Becker, S., Pontasch, S., Dove, S., Hoegh-Guldberg, O., et al. (2015). Differential coral bleaching–contrasting the activity and response of enzymatic antioxidants in symbiotic partners under thermal stress. *Comp. Biochem. Physiol. Part A: Mol. Integr. Physiol.* 190, 15–25. doi: 10.1016/j.cbpa.2015.08.012

LaJeunesse, T. C., Parkinson, J. E., Gabrielson, P. W., Jeong, H. J., Reimer, J. D., Voolstra, C. R., et al. (2018). Systematic revision of symbiodiniaceae highlights the antiquity and diversity of coral endosymbionts. *Curr. Biol.* 28, 2570–2580.e6. doi: 10.1016/j.cub.2018.07.008

Lee, S. S., Song, W., Cho, M., Puppala, H. L., Nguyen, P., Zhu, H., et al. (2013). Antioxidant properties of cerium oxide nanocrystals as a function of nanocrystal diameter and surface coating. *ACS Nano* 7, 9693–9703. doi: 10.1021/nn4026806

Lesser, M. P. (2011). ""Coral bleaching: causes and mechanisms,"," in *Coral reefs: an ecosystem in transition* (Dordrecht: Springer), 405–419.

Levasseur, M., Thompson, P. A., and Harrison, P. J. (1993). Physiological acclimation of marine phytoplankton to different nitrogen sources. *J. Phycol.* 29, 587–595. doi: 10.1111/j.0022-3646.1993.00587.x

Lew, T. T. S., Wong, M. H., Kwak, S.-Y., Sinclair, R., Koman, V. B., and Strano, M. S. (2018). Rational design principles for the transport and subcellular distribution of nanomaterials into plant protoplasts. *Small* 14, 1802086. doi: 10.1002/smll.201802086

Lucas, A. J., Dupont, C. L., Tai, V., Largier, J. L., Palenik, B., and Franks, P. J. (2011). The green ribbon: Multiscale physical control of phytoplankton productivity and community structure over a narrow continental shelf. *Limnol. Oceanogr.* 56, 611–626. doi: 10.4319/lo.2011.56.2.0611

Mansfield, K. M., and Gilmore, T. D. (2019). Innate immunity and cnidarian-symbiodiniaceae mutualism. *Dev. Comp. Immunol.* 90, 199–209. doi: 10.1016/j.dci.2018.09.020

Marla, S. S., Lee, J., and Groves, J. T. (1997). Peroxynitrite rapidly permeates phospholipid membranes. *Proc. Natl. Acad. Sci. U.S.A.* 94, 14243. doi: 10.1073/pnas.94.26.14243

McClanahan, T. R., Ateweberhan, M., Muhando, C. A., Maina, J., and Mohammed, M. S. (2007). Effects of climate and seawater temperature variation on coral bleaching and mortality. *Ecol. Monogr.* 77, 503–525. doi: 10.1890/06-1182.1

Mohammadi, M. H. Z., Panahirad, S., Navai, A., Bahrami, M. K., Kulak, M., and Gohari, G. (2021). Cerium oxide nanoparticles (CeO2-NPs) improve growth parameters and antioxidant defense system in Moldavian balm (Dracocephalum moldavica l.) under salinity stress. *Plant Stress* 1, 100006. doi: 10.1016/j.stress.2021.100006

Moheimani, N. R., Borowitzka, M. A., Isdepsky, A., and Sing, S. F. (2013). "Standard methods for measuring growth of algae and their CompositionAlgae for biofuels and energy," in *Algae for biofuels and energy developmetns in applied phycology* (Dordrecht: Springer). doi: 10.1007/978-94-007-5479-9_16

Motone, K., Takagi, T., Aburaya, S., Aoki, W., Miura, N., Minakuchi, H., et al. (2018). Protection of coral larvae from thermally induced oxidative stress by redox nanoparticles. *Mar. Biotechnol.* 20, 542–548. doi: 10.1007/s10126-018-9825-5

Motone, K., Takagi, T., Aburaya, S., Miura, N., Aoki, W., and Ueda, M. (2020). A zeaxanthin-producing bacterium isolated from the algal phycosphere protects coral endosymbionts from environmental stress. *mBio* 11, e01019–e01019. doi: 10.1128/mBio.01019-19

Navarro, E., Baun, A., Behra, R., Hartmann, N. B., Filser, J., Miao, A.-J., et al. (2008). Environmental behavior and ecotoxicity of engineered nanoparticles to algae, plants, and fungi. *Ecotoxicology* 17, 372–386. doi: 10.1007/s10646-008-0214-0

Nelson, B. C., Johnson, M. E., Walker, M. L., Riley, K. R., and Sims, C. M. (2016). Antioxidant cerium oxide nanoparticles in biology and medicine. *Antioxidants* 5, 15. doi: 10.3390/antiox5020015

Newkirk, G. M., Wu, H., Santana, I., and Giraldo, J. P. (2018). Catalytic scavenging of plant reactive oxygen species *In vivo* by anionic cerium oxide nanoparticles. *JoVE*, e58373. doi: 10.3791/58373

Oliver, T. A., and Palumbi, S. R. (2011). Do fluctuating temperature environments elevate coral thermal tolerance? *Coral Reefs* 30, 429–440. doi: 10.1007/s00338-011-0721-y

Parankusam, S., Adimulam, S. S., Bhatnagar-Mathur, P., and Sharma, K. K. (2017). Nitric oxide (NO) in plant heat stress tolerance: Current knowledge and perspectives. *Front. Plant Sci.* 8. doi: 10.3389/fpls.2017.01582

Peixoto, R. S., Rosado, P. M., Leite, D. C., de, A., Rosado, A. S., and Bourne, D. G. (2017). Beneficial microorganisms for corals (BMC): Proposed mechanisms for coral health and resilience. *Front. Microbiol.* 8. doi: 10.3389/fmicb.2017.00341

Peng, S.-E., Wang, Y.-B., Wang, L.-H., Chen, W.-N. U., Lu, C.-Y., Fang, L.-S., et al. (2010). Proteomic analysis of symbiosome membranes in cnidaria–dinoflagellate endosymbiosis. *Proteomics* 10, 1002–1016. doi: 10.1002/pmic.200900595

Perez, S., and Weis, V. (2006). Nitric oxide and cnidarian bleaching: an eviction notice mediates breakdown of a symbiosis. *J. Exp. Biol.* 209, 2804–2810. doi: 10.1242/jeb.02309

Rädecker, N., Pogoreutz, C., Gegner, H. M., Cárdenas, A., Roth, F., Bougoure, J., et al. (2021). Heat stress destabilizes symbiotic nutrient cycling in corals. *Proc. Natl. Acad. Sci.* 118, e2022653118. doi: 10.1073/pnas.2022653118

Radi, R. (2018). Oxygen radicals, nitric oxide, and peroxynitrite: Redox pathways in molecular medicine. *Proc. Natl. Acad. Sci. U.S.A.* 115, 5839. doi: 10.1073/pnas.1804932115

Rico, C. M., Hong, J., Morales, M. I., Zhao, L., Barrios, A. C., Zhang, J.-Y., et al. (2013). Effect of cerium oxide nanoparticles on rice: a study involving the antioxidant defense system and *in vivo* fluorescence imaging. *Environ. Sci. Technol.* 47, 5635–5642. doi: 10.1021/es401032m

Roger, L. M., Reich, H. G., Lawrence, E., Li, S., Vizgaudis, W., Brenner, N., et al. (2021). Applying model approaches in non-model systems: A review and case study on coral cell culture. *PloS One* 16, e0248953. doi: 10.1371/journal.pone.0248953

Rosado, P. M., Leite, D. C., Duarte, G. A., Chaloub, R. M., Jospin, G., da Rocha, U. N., et al. (2019). Marine probiotics: increasing coral resistance to bleaching through microbiome manipulation. *ISME J.* 13, 921–936. doi: 10.1038/s41396-018-0323-6

Rosic, N. N., Leggat, W., Kaniewska, P., Dove, S., and Hoegh-Guldberg, O. (2013). New-old hemoglobin-like proteins of symbiotic dinoflagellates. *Ecol. Evol.* 3, 822–834. doi: 10.1002/ece3.498

Rosset, S. L., Oakley, C. A., Ferrier-Pagès, C., Suggett, D. J., Weis, V. M., and Davy, S. K. (2021). The molecular language of the cnidarian–dinoflagellate symbiosis. *Trends Microbiol.* 29, 320–333. doi: 10.1016/j.tim.2020.08.005

Szabó, C., Ischiropoulos, H., and Radi, R. (2007). Peroxynitrite: biochemistry, pathophysiology and development of therapeutics. *Nat. Rev. Drug Discov.* 6, 662–680. doi: 10.1038/nrd2222

Thies, A. B., Quijada-Rodriguez, A. R., Zhouyao, H., Weihrauch, D., and Tresguerres, M. (2022). A rhesus channel in the coral symbiosome membrane suggests a novel mechanism to regulate NH3 and CO2 delivery to algal symbionts. *Sci. Adv.* 8, eabm0303. doi: 10.1126/sciadv.abm0303

Turner, M. G., Calder, W. J., Cumming, G. S., Hughes, T. P., Jentsch, A., LaDeau, S. L., et al. (2020). Climate change, ecosystems and abrupt change: science priorities. *Philos. Trans. R. Soc. B* 375, 20190105. doi: 10.1098/rstb.2019.0105

Vandelle, E., and Delledonne, M. (2011). Peroxynitrite formation and function in plants. *Plant Sci.* 181, 534–539. doi: 10.1016/j.plantsci.2011.05.002

Van Hoecke, K., De Schamphelaere, K. A., van der Meeren, P., Smagghe, G., and Janssen, C. R. (2011). Aggregation and ecotoxicity of CeO2 nanoparticles in synthetic and natural waters with variable pH, organic matter concentration and ionic strength. *Environ. pollut.* 159, 970–976. doi: 10.1016/j.envpol.2010.12.010

van Oppen, M. J. H., and Lough, J. M. (2018). ""Synthesis: Coral bleaching: Patterns, processes, causes and consequences,"," in *Coral bleaching: Patterns, processes, causes and consequences*. Eds. M. J. H. van Oppen and J. M. Lough (Cham: Springer International Publishing), 343–348. doi: 10.1007/978-3-319-75393-5_14

van Oppen, M. J. H., Oliver, J. K., Putnam, H. M., and Gates, R. D. (2015). Building coral reef resilience through assisted evolution. *Proc. Natl. Acad. Sci. U.S.A.* 112, 2307. doi: 10.1073/pnas.1422301112

Wang, F., Guan, W., Xu, L., Ding, Z., Ma, H., Ma, A., et al. (2019). Effects of nanoparticles on algae: Adsorption, distribution, ecotoxicity and fate. *Appl. Sci.* 9, 1534–1549. doi: 10.3390/app9081534

Weis, V. M. (2008). Cellular mechanisms of cnidarian bleaching: stress causes the collapse of symbiosis. *J. Exp. Biol.* 211, 3059–3066. doi: 10.1242/jeb.009597

Wong, M. H., Misra, R. P., Giraldo, J. P., Kwak, S.-Y., Son, Y., Landry, M. P., et al. (2016). Lipid exchange envelope penetration (LEEP) of nanoparticles for plant engineering: A universal localization mechanism. *Nano Lett.* 16, 1161–1172. doi: 10.1021/acs.nanolett.5b04467

Wu, H., Tito, N., and Giraldo, J. P. (2017). Anionic cerium oxide nanoparticles protect plant photosynthesis from abiotic stress by scavenging reactive oxygen species. *ACS Nano* 11, 11283–11297. doi: 10.1021/acsnano.7b05723

Xiang, T., Hambleton, E. A., DeNofrio, J. C., Pringle, J. R., and Grossman, A. R. (2013). Isolation of clonal axenic strains of the symbiotic dinoflagellate symbiodinium and their growth and host specificity1. *J. Phycol.* 49, 447–458. doi: 10.1111/jpy.12055

Zhao, J., and Riediker, M. (2014). Detecting the oxidative reactivity of nanoparticles: a new protocol for reducing artifacts. *J. Nanopart. Res.* 16, 1–13. doi: 10.1007/s11051-014-2493-0